Joint CI-JAI advanced accelerator lecture series

Imaging and detectors for medical physics

Lecture 7: PET

Dr Barbara Camanzi

barbara.camanzi@stfc.ac.uk

UNIVERSITY OF OXFORD

Course layout

Day	AM 09.30 – 11.00	PM 15.30 – 17.00
Week 1		
6th June	Lecture 1: Introduction to medical imaging	Lecture 2: Detectors for medical imaging
7th June	Lecture 3: X-ray imaging	
8th June		Tutorial
Week 2		
13th June	Lecture 4: Radionuclides	
14th June	Lecture 5: Gamma cameras	Lecture 6: SPECT
16th June	Lecture 7: PET	
Week 3		
22nd June	Tutorial	

UNIVERSITY OF OXFORD

Books

1. N Barrie Smith & A Webb
   Introduction to Medical Imaging
   Cambridge University Press

2. Edited by M A Flower
   Webb's Physics of Medical Imaging
   CRC Press

3. A Del Guerra
   Ionizing Radiation Detectors for Medical Imaging
   World Scientific

4. W R Leo
   Techniques for Nuclear and Particle Physics Experiments
   Springer-Verlag

Positron Emission Tomography (PET)

Ref. 1 – Chapters 3.13 to 3.21

- Tomographic technique that uses radiotracers administered to the patient → emission imaging
- Basic principle:
  1. Radiotracers used undergo β^+ decay → emit e^+
  2. e^+ travels on average $0.1 \div 3$ mm in tissue depending on radiotracer → scatters → loses energy → comes to rest
  3. e^+ at rest combines with atomic e^- to form positronium
  4. Positronium decays emitting two back-to-back 511 keV γ-rays

β^+ decay

- Proton-rich or neutron deficient radionuclide ejects β^+-particle = e^+ = +1 charge in the process:

$$p \rightarrow n + e^+ + \nu$$

- Three-body decay $\rightarrow$ energy spectrum of e^+ = continuum up to a maximum
- $Z \rightarrow Z - 1,\ A$ and atomic weight remain the same

Example

$$^{15}_{8}O \xrightarrow{\beta^+\text{decay}} {}^{15}_{7}N + \beta^+ + \nu + E$$

E = shared randomly between ν and kinetic energy of β^+

Average kinetic energy $\langle E_{\beta^+} \rangle \cong E_{\beta^+}^{max}/3$

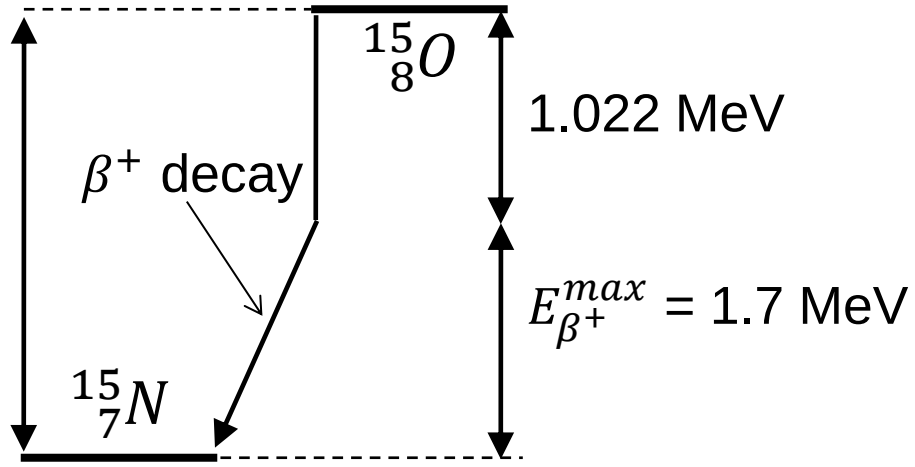

Common radiotracers for PET

Radionuclide Radiotracer	Half-life (min)	β^+ fraction	Max . kinetic energy (Mev)	Average β^+ range in water (mm)	Clinical application
^{11}C ^{11}C-palmitate	20.4	0.99	0.96	1.0	Cardiac metabolism
^{13}N $^{13}NH_3$	9.96	1.00	1.19	2.0	Cardiac blood flow
^{15}O $H_2{}^{15}O$	2.07	1.00	1.72	2.0	Cerebral blood flow
^{18}F ^{18}FDG	109.7	0.97	0.64	0.6	Oncology, inflammation, cardiac viability
$^{82}Rb^1$ $^{82}RbCl_2$	1.27	0.95	3.35	2.8	Cardiac perfusion

[1]Only radioisotope produced at on-site generator and not cyclotron

^{18}F-fluoro-2-deoxy-D-glucose (FDG)

- Most common radiotracer used in 80% of PET studies
- FDG injected into blood stream → transported to cells across body

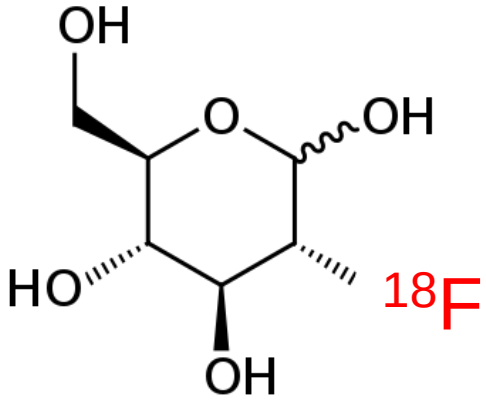

- Uptake depends on rate of glucose utilization = glucose metabolism:
  - High glucose metabolic rate characteristic of many tumours → hot spots in oncological PET scans

PET –vs– SPECT

- Main difference:
  - Two γ-rays (PET) instead of one (SPECT)

Advantages
Much higher SNR_{PET} arises from: 1. Collimation not required → no absorption of γ-rays 2. Higher E_{γ}^{PET} → less γ-rays attenuation in tissue 3. Use of complete ring of detectors
Significantly better spatial resolution
Two back-to-back γ-rays → two signals in the ring of detectors → two points → intrinsic line-of-response (LOR) → no collimation needed to select directions
Disadvantages
(On-site) cyclotron needed to produce β^+ emitters
High associated cost

PET components

- Detection unit = full ring of scintillating detectors surrounding the patient
- Scintillation read-out chain:
  - PMTs → convert light into electric signal
  - Pulse height analyzer
- Annihilation coincidence detection unit

Scintillating detector ring

- Large number of small scintillation crystals placed in circular ring surrounding patient with diameter:
  - 70 or 85 cm for abdominal scanner
  - ~45 cm for head scanner
- Up to 48 multiple rings staked axially with retractable lead collimation septa in between → head/foot FOV = ~16 cm
- Ideal geometry = one crystal coupled to one PMT → better spatial resolution but too expensive
- Geometry = 'block detector' design

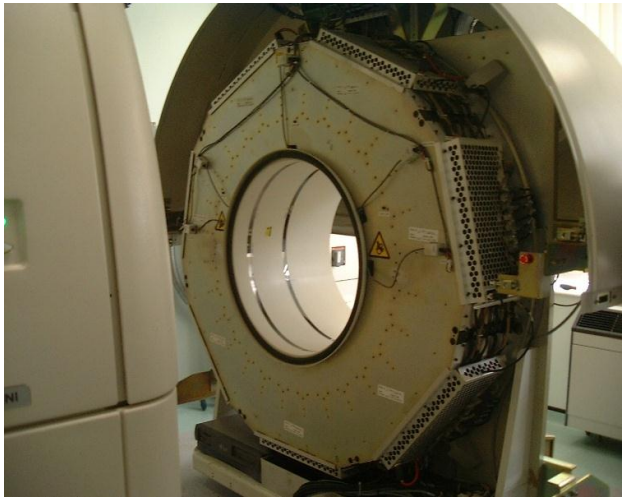

Courtesy Mike Partridge (Oxford)

‘Block detector’ design

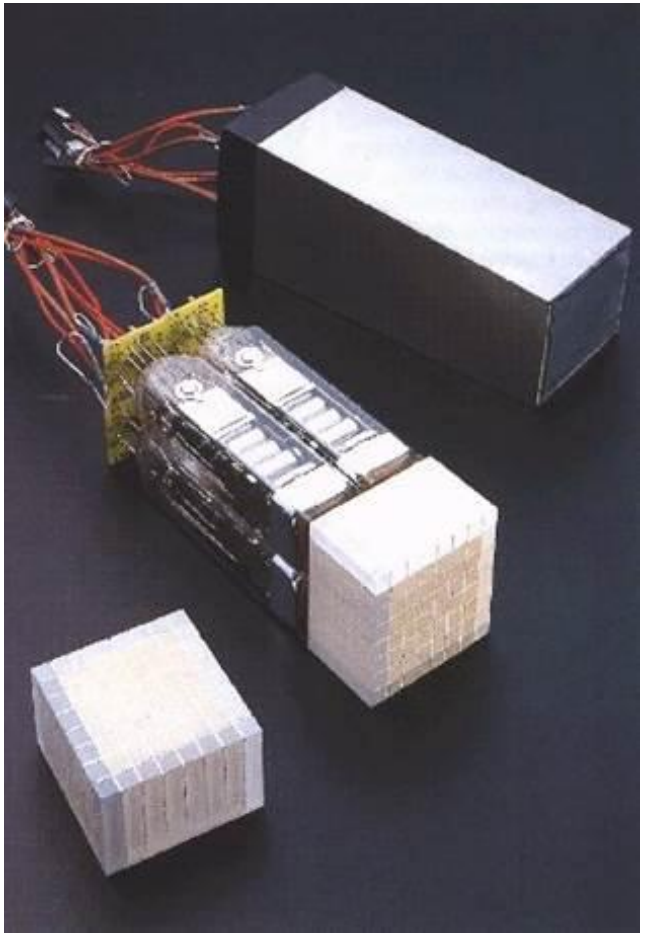

Courtesy Mike Partridge (Oxford)

- Large block of scintillating material $\sim 50 \times 50 \times 30\ \mathrm{cm}^3$
- Partial cuts through filled with reflective material → prevent light formed at top of crystal to produce very broad LSF while travelling 30 cm to PMT

‘Block detector’ geometry

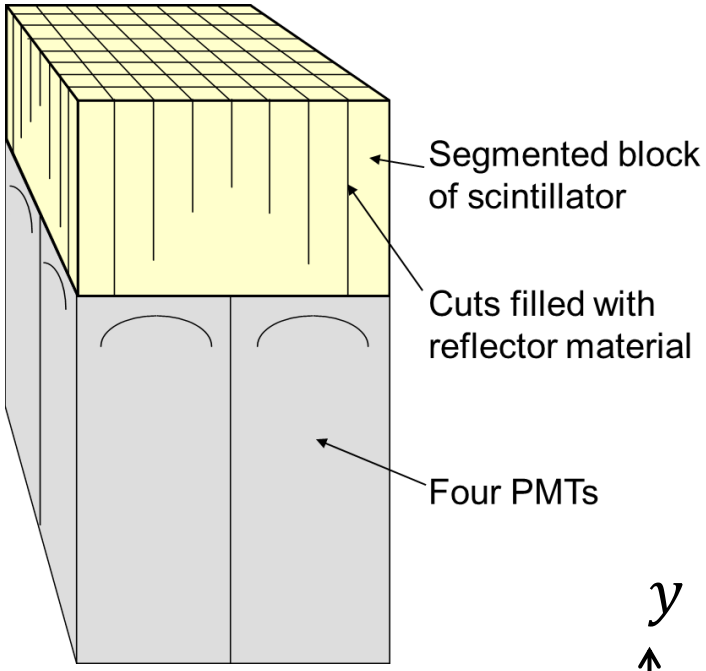

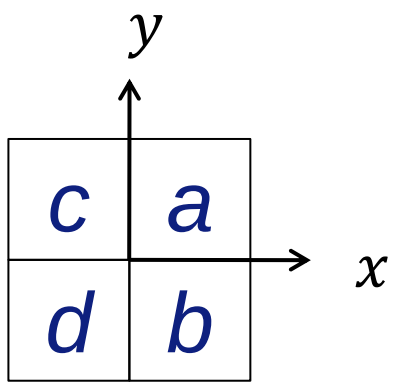

Courtesy Piero Posocco (Imperial College)

- Geometry = 8×8 array of cuts $\rightarrow$ 64 ‘crystals’ of $\sim 6 \times 6\ \mathrm{cm}^2$ area and 30 cm length coupled to 4 PMTs $\rightarrow$ multiplexing factor of 16
- The X-Y position measured relative to the centre of the block of four PMTs is:

$$X = \frac{(a + b - c - d)}{(a + b + c + d)}$$

$$Y = \frac{(a - b + c - d)}{(a + b + c + d)}$$

Scintillation crystals

- Ideal scintillation material for use in PET has:
  1. High detection efficiency for 511 keV γ-rays
  2. Short decay time to allow for short coincidence resolving time
  3. High light yield to reduce the complexity and cost of the system
  4. Emission wavelength near 400 nm that corresponds to maximum sensitivity for standard PMTs
  5. Optical transparency at emission wavelength to minimise reabsorption
  6. Index of refraction close to 1.5 to ensure efficient light transmission between crystal and PMT

Common scintillator materials for PET

	Decay time (ns)	Relative light yield[1]	Efficiency	Emission wavelength (nm)	Refractive index
BGO	300	0.15	0.72	480	2.15
$LSO(Ce)$	40	0.75	0.69	420	1.82
BaF_2	0.8 prim 600 sec	0.12	0.34	220, 310	1.49
$GSO(Ce)$	60 prim 600 sec	0.3	0.57	430	1.85
$NaI(Tl)$	230 prim 10^4 sec	1.0	0.24	410	1.85

[1]Relative to $NaI(Tl)$

- Scintillator must be 2 cm or more in thickness for high sensitivity
- $NaI(Tl)$ =low efficiency for 511 keV γ-rays $\rightarrow$ not used in PET

Scintillation read-out chain

PMTs

- Standard operation → scintillation light = optical photons converted into an amplified electric signal by the PMTs

Pulse height analyzer

- Multi-channel analyser receives in input the PMT signal and converts it into a ‘logic pulse’ typically $6 \div 10$ ns long if PMT signal amplitude is within pre-set range
- ‘Logic pulse’ sent to coincidence unit

Data acquisition

- Two different modes:
  1. 2D multi-slice mode
  2. Full 3D mode → becoming more common due to far superior SNR

2D

- Collimation septa extended

3D

- Collimation septa retracted
- Requires fully 3D reconstruction algorithm

2D PET –vs– 3D PET

2D

- Advantages:
  1. Reduced amount of scattered γ-rays
  2. Uniform sensitivity profile along axial direction

3D

- Advantages:
  1. Factor 10 higher sensitivity than 2D PET $\rightarrow$ higher SNR
  2. For same SNR as in 2D PET $\rightarrow$ two order magnitude reduction in scan time
- Disadvantages:
  1. More random coincidences and scattered γ-rays
  2. Sensitivity profile in axial direction higher at the centre than at ends

2D PET and 3D PET in whole-body PET

- Whole-body PET = bed is moved several times along head/foot directions to cover entire body length

2D

- Uniform sensitivity profile along axial direction → overlap between successive bed positions = only ~1÷2 cm

3D

- Non-uniform sensitivity profile along axial direction → overlap between successive bed positions = as high as 50% → more bed positions required

2D multi-slice acquisition

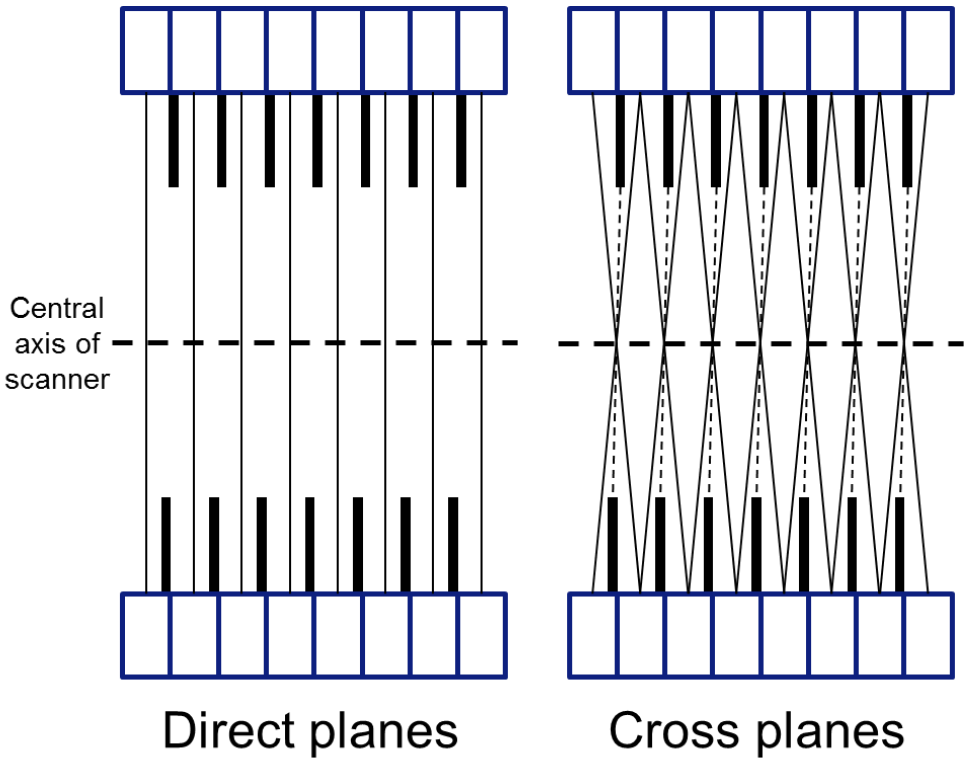

Courtesy Piero Posocco (Imperial College)

- Image planes formed:
  1. Between two crystals in same ring = direct planes
  2. From crystals in adjacent rings = cross planes
- For system with n rings:
  - n direct planes
  - n-1 cross planes
  - Total 2n-1 planes

Full 3D acquisition

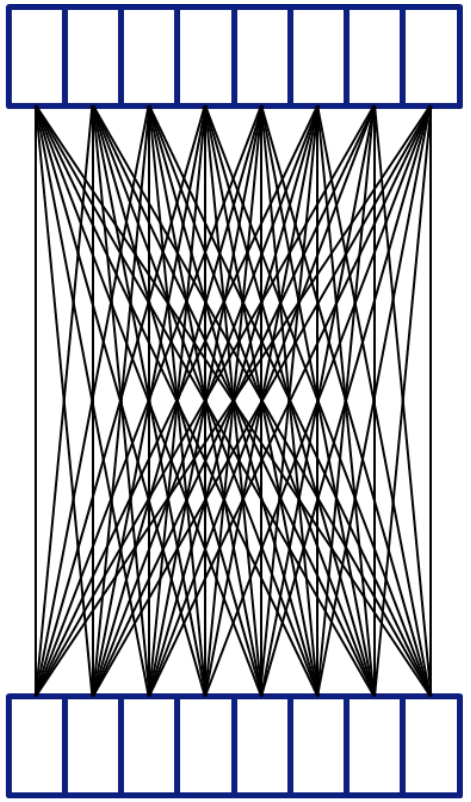

Courtesy Piero Posocco (Imperial College)

- Image planes in a much more complicated configuration

Annihilation coincidence detection unit

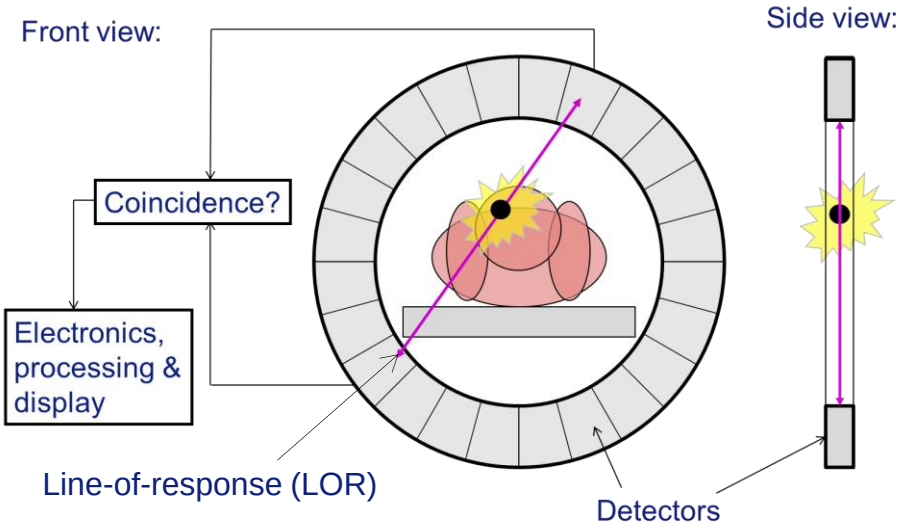

Courtesy Piero Posocco (Imperial College)

- Time
  - Fixed ‘coincidence resolving time’ = time window for each PET system
  - Each signal recorded in a crystal given a time-stamp with precision $1 \div 2$ ns to account for different arrival time of two γ-rays at detector ring
- Position
  - Geometric ‘coincidence arcs’ = two arcs at $180°$ formed by set number of crystals

Annihilation coincidence detection

- Time
  - 1st γ-ray detected at time $t_1 = 0$
  - 2nd γ-ray detected at time t_2
- Position
  - 1st γ-ray detected assigned to crystal 1
  - 2nd γ-ray detected assigned to crystal 2
- Coincidence
  - If t_2 falls into time window $\rightarrow$ 2nd γ-ray assigned to same annihilation
  - If crystals 1 and 2 are operated in coincidence $\rightarrow$ two γ-rays accepted as 'true event' and LOR drawn

Types of coincidence events in PET

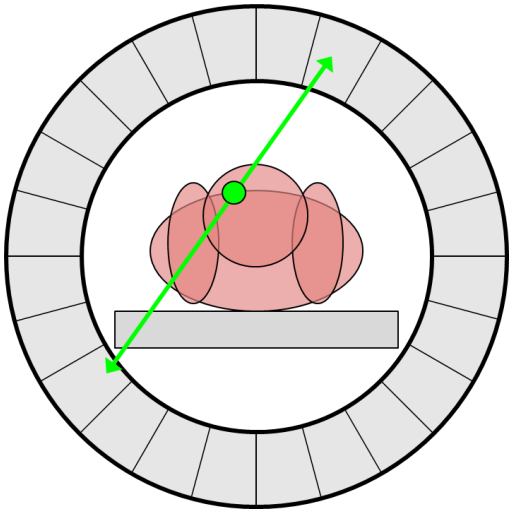

True

Both γ-rays escape without scatter and interact in detectors

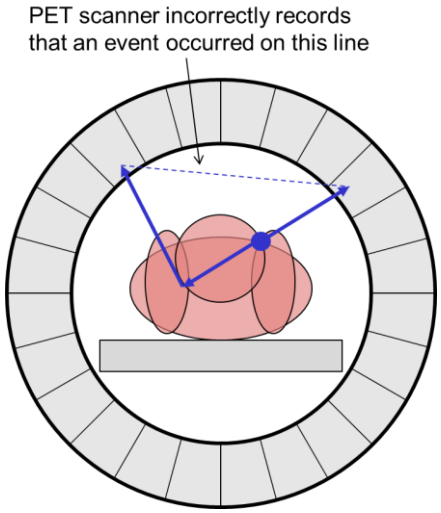

Scatter

One or both γ-rays scatter in tissue

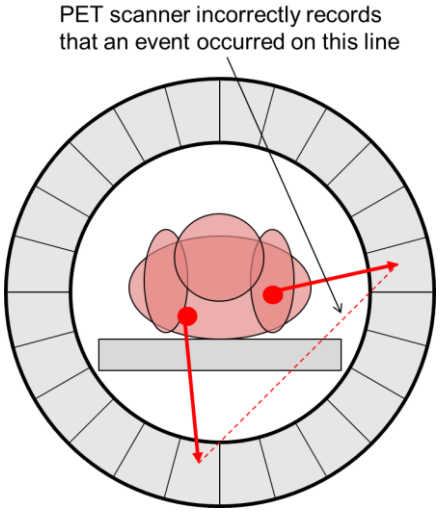

Random (accidental)

Two γ-rays from separate emissions strike the detectors at the same time

Scatter events

- Two main sources of scatter:
  1. Within the body
  2. Within the scintillator
- Leads to reduction in image contrast

Scatter contribution

- High contribution due to:
  1. Only one of two annihilation γ-rays has to scatter
  2. BGO and LSO poor intrinsic energy resolution compared to $NAI(Tl)$ = cannot discriminate scattered from unscattered γ-rays $\rightarrow$ scatter events significant fraction
     1. Ex: detection window for BGO 450-650 keV while γ-ray scattered at 45° loses only ~115 keV
  3. Higher in 3D PET due to elimination of collimator

2D	3D
$10 \div 15\%$	Up to 50%

Random coincidences

- Random coincidences are due to two separate disintegrations occurring very close in time
- Uniformly distributed across FOV → significant errors in areas of very low activity
- Rate $R_{randoms}$ for a time window τ is given by:

$$R_{randoms} = R_{S_i} \times R_{S_j} \times 2\tau$$

R_{s_n} = detection rate at scintillation detector n

- Contribution:
  - For head scanners $\sim 20\%$
  - For body scanners close to 50%

Image formation

- Two steps:
  1. Correction of data for:
     a. Attenuation effects
     b. Scatter
     c. Accidental and multiple coincidences
     d. Dead-time
  2. Tomographic image reconstruction = SPECT → CT reconstruction methods:
     a. Filtered backprojection method
     b. Iterative method

Attenuation correction

- Old method (pre PET/CT)

  Identical to SPECT = transmission-based calibration with ^{68}Ge used to estimate attenuation

- Current method (PET/CT)

  CT images segmented according tissue type[1] → standard value of μ at 511 keV assigned → attenuation map smoothed to match PET resolution and applied to PET image

[1]Muscle, lipid, bone, etc.

Scatter correction

- Three different approaches:
  1. Background subtraction approach → simplest method
     a. Measure signal intensity outside the patient → fit values to a Gaussian to estimate amount of scatter in patient = function
     b. Function subtracted from raw data → corrected image
     c. Works well for homogeneous organs (brain) but not abdomen
  2. Dual-energy window approach
     a. Two options:
        i. Lower window $190 \div 350$ keV + upper window $350 \div 650$ keV
        ii. Lower window $450 \div 650$ keV + upper window $550 \div 650$ keV → overlap = Estimation of trues method (ETM)
     b. Scatter data scaled appropriately and subtracted from data in photopeak window → corrected image
  3. Iterative reconstruction approach
     a. Uses simulations and CT-derived attenuation maps
     b. Most sophisticated, computationally intensive and time-consuming

Random coincidences corrections

- Two methods:
  1. Use of additional parallel timing circuitry = most common
     a. Second time window starts typically 60 ns after event is recorded
     b. Standard window measures total number of coincidences + delayed window records only random events → subtracted from total
  2. Use relation between $R_{randoms}$ and R_{S_i}
     a. Measured values of R_{S_i} used to determine $R_{randoms}$ → subtracted from acquired data

Multiple coincidences corrections

- Multiple = more than two events recorded during one time window
- One method:
  1. Total number of multiple coincidences $R_{multiple}$ estimated as:

$$R_{multiple} \approx R_{randoms} \times R_{S_i} \times R_{S_j} \times \tau$$

  2. Multiple event coincidences discarded before image reconstruction

Dead-time

- Maximum count rate the system can record due to components' finite response and recovery time
- Fractional dead time = ratio of measured count rate to theoretical count rate with zero dead-time
- Major sources of dead-time in PET:
  1. Time taken to integrate the charge from the PMTs
  2. Processing time of a coincidence event
  3. Multiple coincidences → data are discarded
- Corrections performed by:
  1. Characterising the dead-time of each component
  2. Estimating the number of multiple coincidences expected

Sensitivity

- True coincidence count rate R_{true} for a β^+-emitter in air near midpoint between pair of detectors is:

$$R_{true} = R_{e^+}\varepsilon^2(2G)$$

$R_{e^+}[s^{-1}]$ = rate of e^+

$\varepsilon = \frac{N^{\gamma}_{recorded}}{N^{\gamma}_{hitting}}$ = intrinsic detector efficiency

$G = \frac{A}{4\pi r^2}$ = geometric efficiency of individual detector of effective area A and radius r

- Determined primarily by detector efficiency and solid angle coverage

Signal-to-noise ratio

- Factors affecting SNR:
  1. Dose administered to patient
  2. Targeting efficiency
  3. γ-ray attenuation in body $\rightarrow$ lower than in SPECT due to higher E_γ
  4. System sensitivity $\rightarrow$ greater than in SPECT due to lack of collimator and higher E_γ

	SPECT	2D PET	3D PET
γ-rays detected	$0.01 \div 0.03\%$	$0.2 \div 0.5\%$	$2 \div 10\%$

  5. Image acquisition time
  6. Image post-processing

Contrast-to-noise ratio

- Factors affecting CNR:
  1. Same factors affecting SNR
  2. Non-specific uptake of radiotracer in healthy tissues surrounding pathology being studied
  3. Corrections for Compton scattered γ-rays

Spatial resolution

- Factors affecting the spatial resolution:
  1. Effective e^+ range in tissue $\rightarrow \delta R_{range}$
  2. Non-colinearity of two γ-rays $\rightarrow \delta R_{180^\circ}$
  3. Dimension of the scintillating crystals $\rightarrow \delta R_{detector}$
- Overall spatial resolution δR_{sys} given by:

$$\delta R_{sys} = \sqrt{\delta R_{range}^2 + \delta R_{180^\circ}^2 + \delta R_{detector}^2}$$

- 'Double detection' of two γ-rays reduces depth dependence of $PSF \rightarrow$ spatial resolution less dependent from depth in body than in SPECT

Effective e^+ range

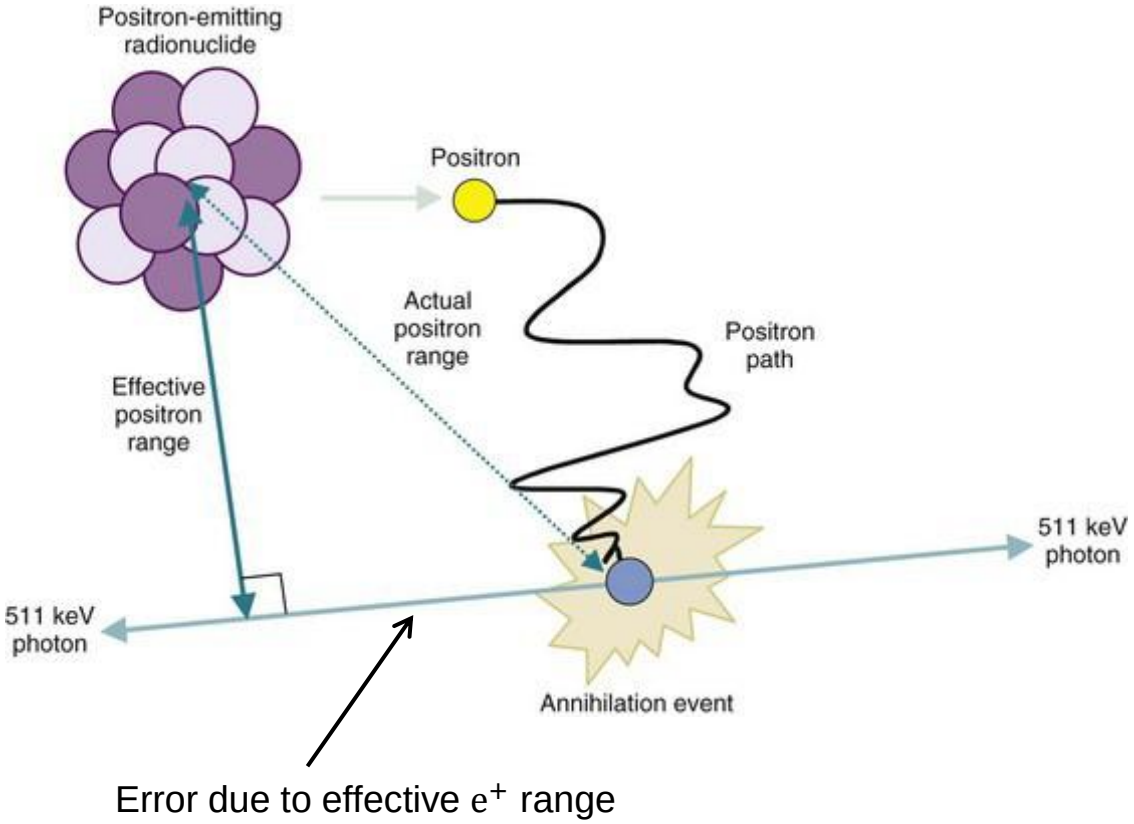

- The e^+ travels a certain distance before coming to rest → effective e^+ range in tissue → error in the determination of the point where e^+ was produced
- This contribution is intrinsic and cannot be eliminated

Effective e^+ range distribution

- Example of an effective e^+ range distribution:

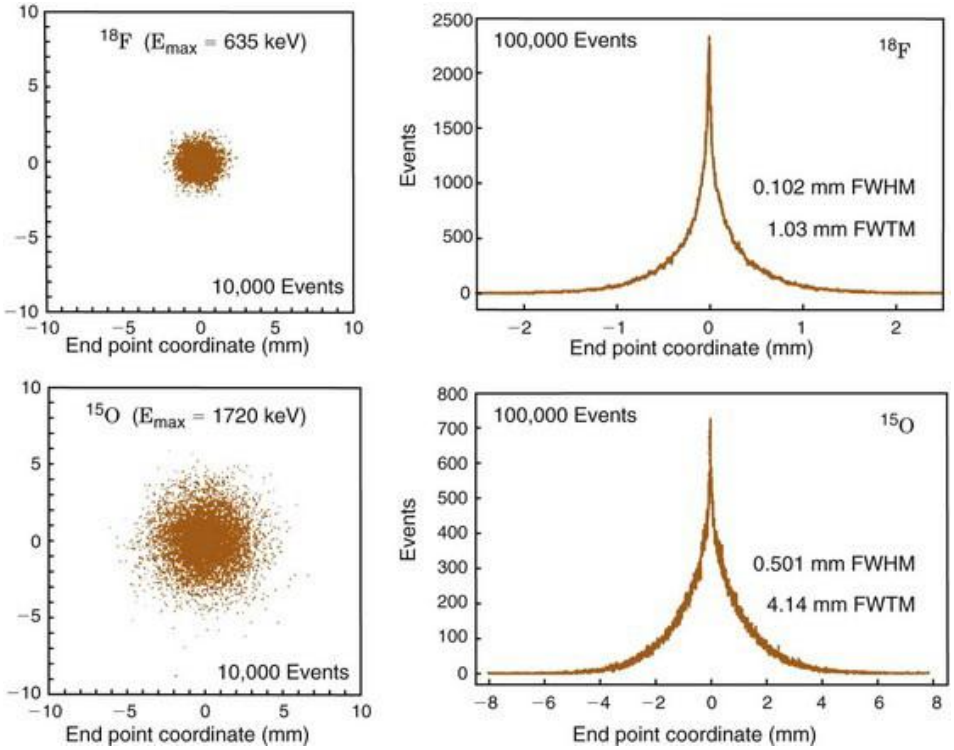

- The distribution is better described by the root mean square rms or σ than $FWHM$

Effect of e^+ range on spatial resolution

- Effective e^+ range increases → spatial resolution decreases with:
  1. Maximum kinetic energy of the emitted e^+ = the higher the energy the longer distance e^+ needs to travel to lose all its energy
  2. The tissue density = the lower the density of the tissue the less interactions e^+ undergoes per unit length → the less energy e^+ loses per unit length → the longer distance e^+ needs to travel to lose all its energy

Non-colinearity

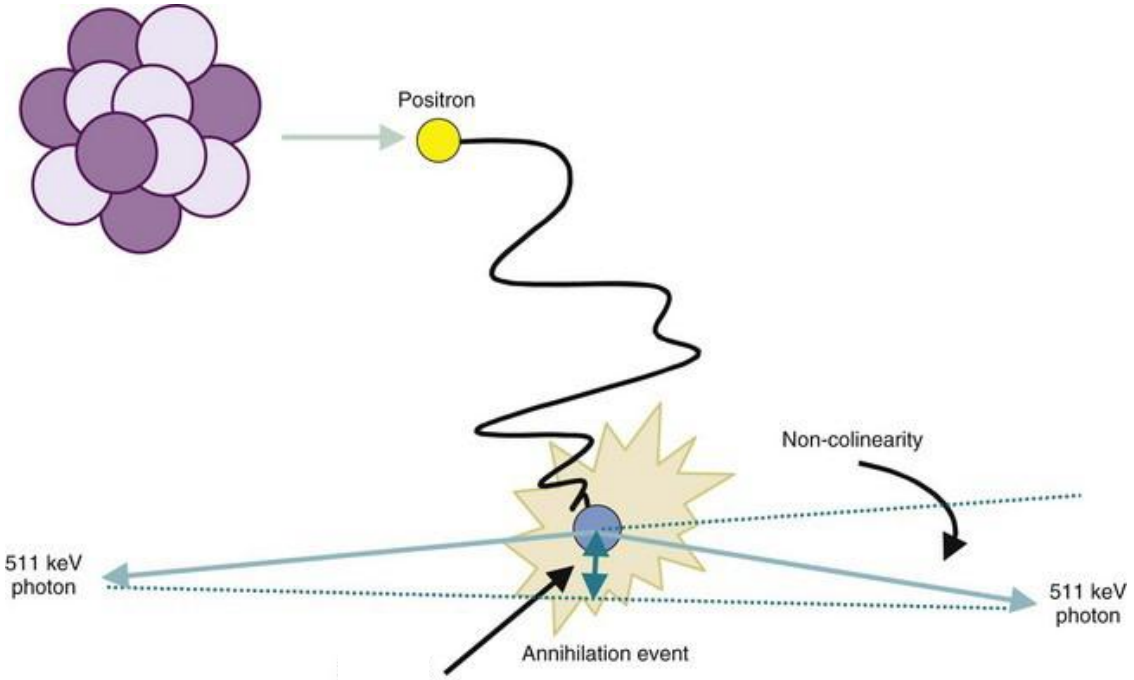

Error due to non-colinearity

- Non-colinearity of two γ-rays = small random deviation from $180°$ angle between two trajectories due to residual motion of e^+ at point of annihilation
- Distribution in angles between two trajectories centred around $180°$ and has $FWHM \cong 0.5°$

Effect of non-colinearity on spatial resolution

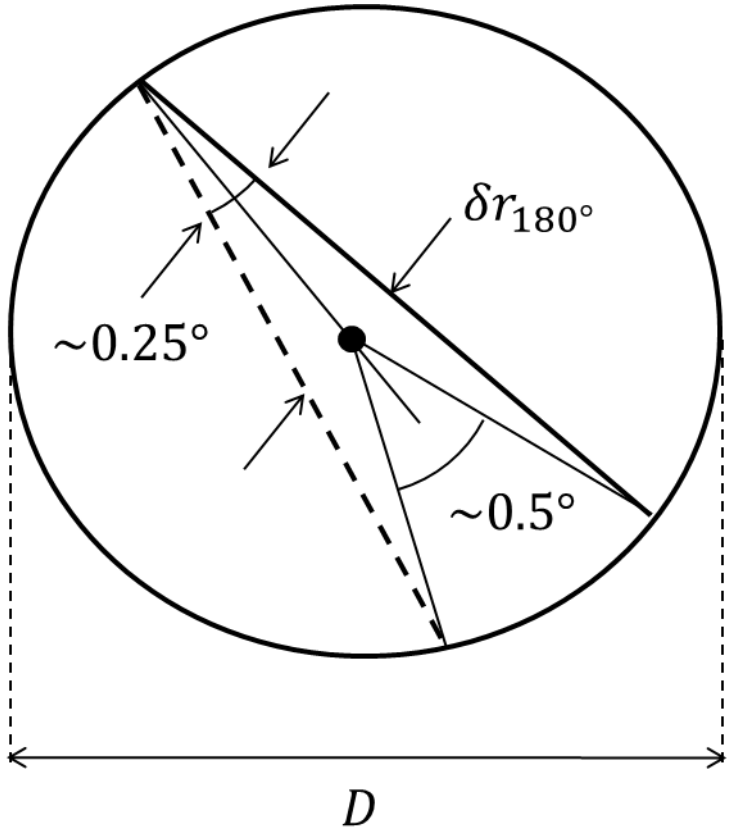

- The larger the diameter of the detector ring the greater the effect on the spatial resolution

$$\delta r_{180°} = \frac{D}{2} \times \frac{0.25\pi}{180}$$
$$= 0.0022 \times D$$

D = diameter of the PET scanner

Effect of scintillating crystals dimension on spatial resolution

- The smaller the scintillating crystals the better the spatial resolution due to:
  1. Area = the spatial resolution decreases with area = given approximately by half the crystal diameter

     The precision in locating the position = spatial resolution at which the γ-ray reaches the scanner increases for crystals with smaller area
  2. Length = the spatial resolution decreases with length
     The uncertainty in the depth-of-interaction (DOI) = point within the crystal where the γ-ray is absorbed and creates scintillation increases for longer crystals $\rightarrow$ the spatial resolution decreases for longer crystals

Factors affecting the spatial resolution

1. Effective e^+ range in tissue = distance increases with:
2. Non-colinearity of two γ-rays = small random deviation from $180°$ angle between two trajectories $\rightarrow$ distribution around $180°$ with $FWHM \cong 0.5° \rightarrow$ the larger the diameter of the detector ring the greater the effect
3. Dimension of the scintillating crystals $\rightarrow$ spatial resolution given by approximately half the crystal diameter + depth-of-interaction uncertainty increases with length of crystal

Time-Of-Flight (TOF) PET

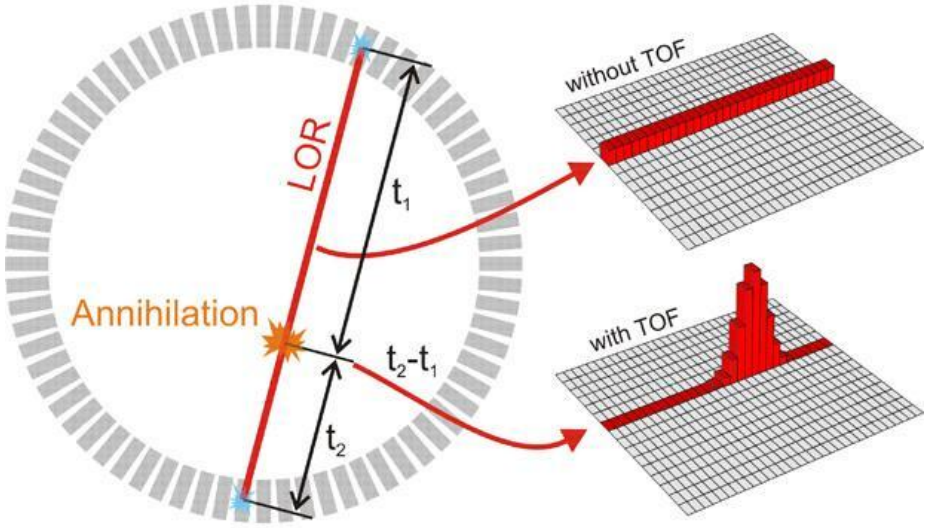

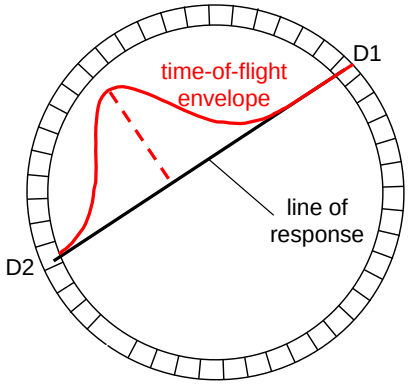

- Very accurate measurement of exact time at which each γ-ray arrives at the detector → localisation within LOR:
  - Time difference between signals from two crystals measured
  - Annihilation point along LOR directly calculated
- Technology for TOF PET:
  - Fast scintillating materials:
    - LSO material of choice: coincidence time = ~ 450 ps instead of 3 ns for BGO
  - Fast photon detectors:
    - SiPMs being investigated

TOF in context

- For a system with timing resolution Δt, the position resolution Δx along LOR is given by:

$$\Delta x = \frac{c\Delta t}{2}$$

  $c =$ speed of light

- Timing resolution of commercial scanners ~ 500 ps
- R&D goals:

Δt (ps)	Δx (cm)
100	3
30	< 1

Advantages of TOF PET

- ~ 500 ps timing resolution $\rightarrow \sim 7.5$ cm spatial resolution $>$ spatial resolution of conventional scanners
- Length of LOR constrained down to ~ 7.5 cm from that of conventional scanners ($\gg 7.5$ cm) $\rightarrow$ statistical noise in the measurement reduced $\rightarrow SNR$ improved
- Noise variance[1] reduction factor f for patient of size D:

$$f = \frac{D}{\Delta x} = \frac{2D}{c\Delta t}$$

- Better $SNR \rightarrow$ higher sensitivity and specificity

[1]Noise variance proportional to length of LOR

Hybrid PET/CT

- Stand-alone PET scanner almost entirely replaced by hybrid PET/CT scanners:
  1. Two separate systems one next to the other
  2. Bed that slides between two systems
- Rationale:
  - Improved attenuation correction
  - Ability to fuse anatomical (morphological) and functional information

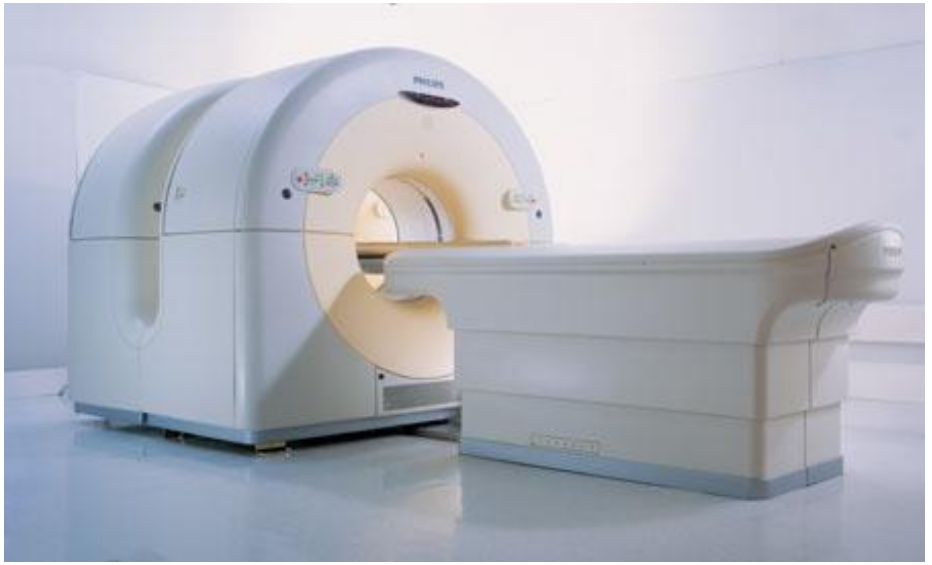

Image fusion in PET/CT

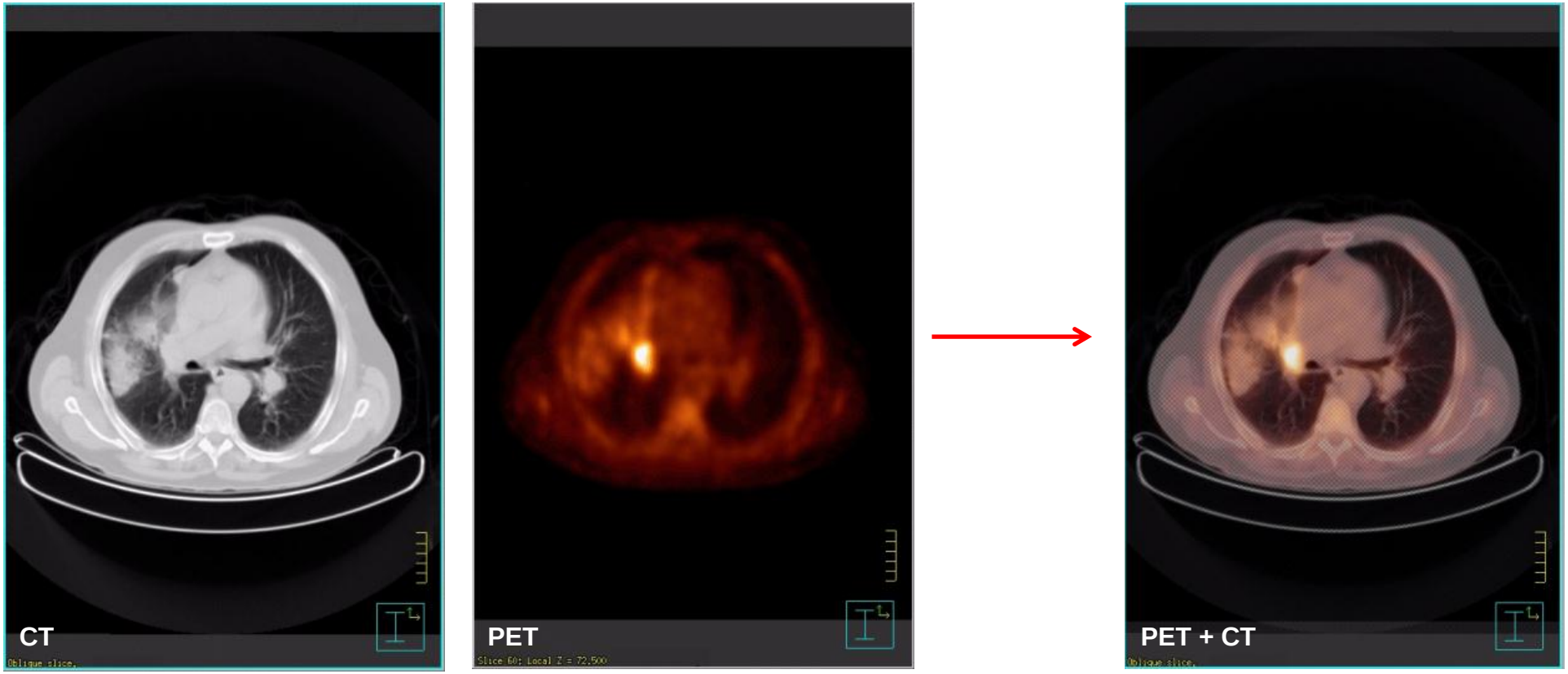

Courtesy Mike Partridge (Oxford)

Clinical applications of PET/CT

- PET/CT scans currently represent ~5÷10% of all nuclear medicine imaging and increase each year
- Clinical investigations:
  1. Oncology (~90% of all investigations)
     - Whole body PET imaging used to identify both primary and secondary metastatic disease away from primary tumour
  2. Cardiology
  3. Neurology

Whole-body PET/CT

- Used in oncology for staging of cancer = determined based on number of secondary lesions = metastases spread away from primary lesion
- Radiotracer used: $FDG \rightarrow$ metabolised more by malignant cells
- Typical scan time $30 \div 60$ min

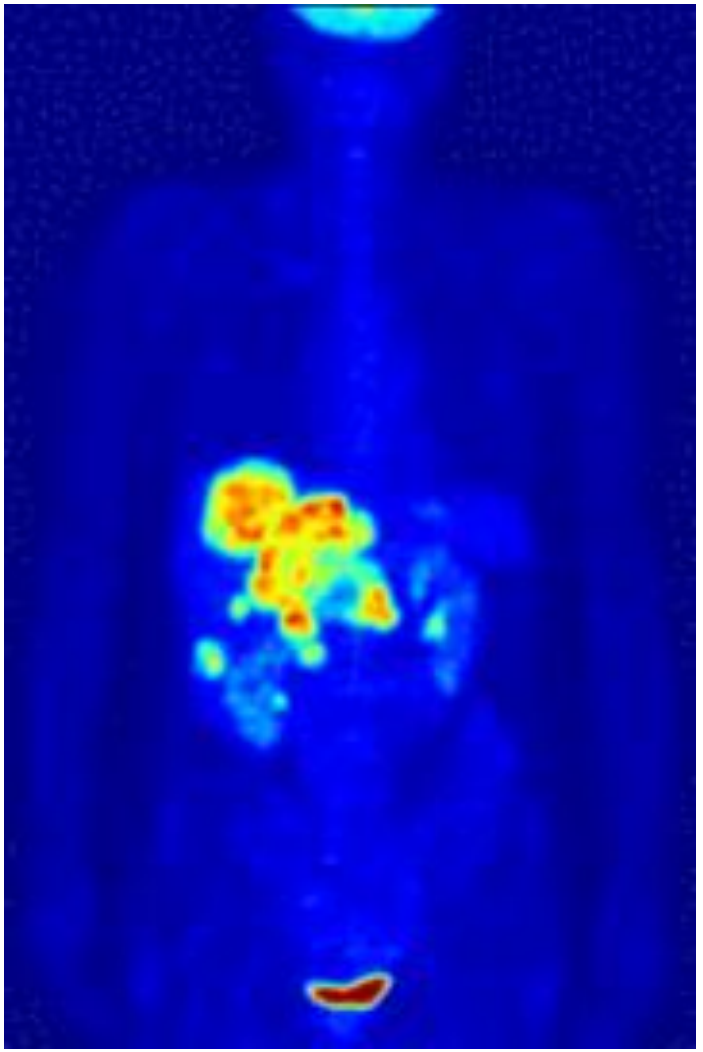

PET/CT in brain imaging

- Used to investigate:
  1. Neurodegenerative dementias such as Alzheimer's (AD) and Parkinson's diseases and distinguish them from from other dementias → AD characterised by low metabolism

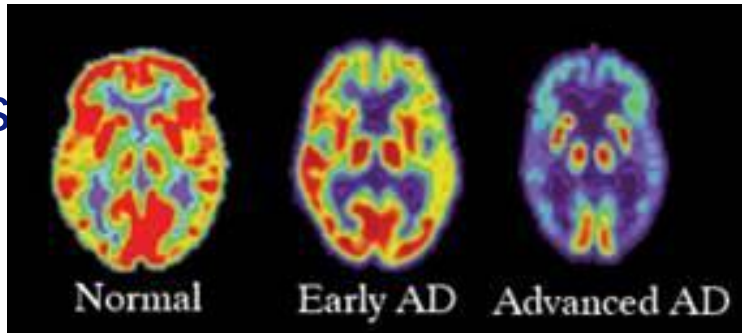

  2. Brain tumours: also to distinguish recurrences from radiation induced necrosis
  3. Trauma
  4. Developmental abnormalities
  5. Epilepsy

Cardiac PET/CT studies

- Used for the study of coronal artery diseases → myocardial viability and perfusion

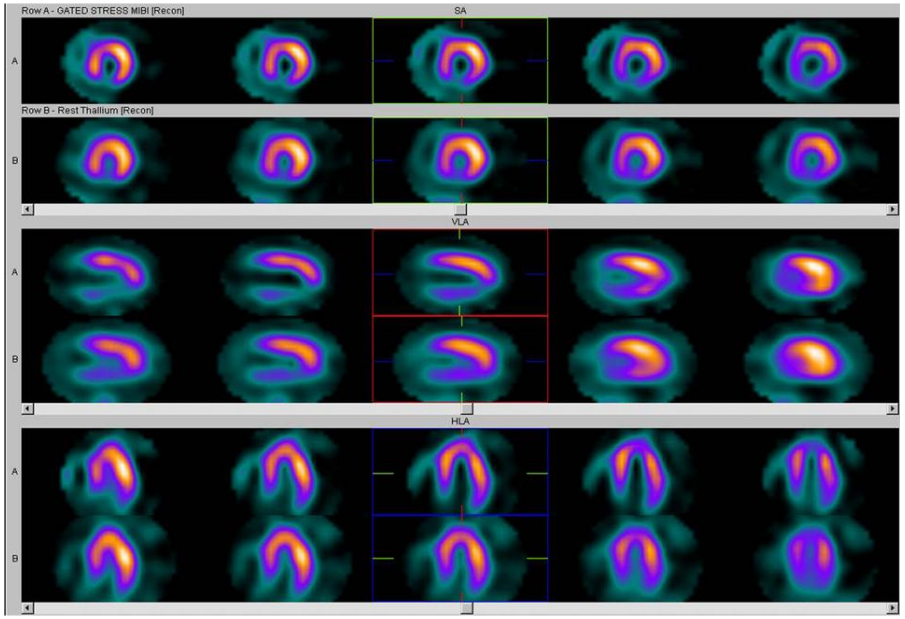

- PET/CT use in cardiac studies is increasing → where available is used instead of SPECT